Using cytoplasmic distribution of phosphorylated tyrosine (pY) residues associated with TCR clusters, we next measured signaling activity specific to each TCR cluster within constrained synapse motifs (*17*) (see also fig. S3). At early time points, pY patterns were similar in both native and repatterned synapses (Fig. 3, A and B). However, at 5 min, TCR clusters in the natively pattered IS were observed only in the c-SMAC region and had very low pY levels (Fig. 3C). In contrast, TCR clusters that had been stably restrained to the periphery of the contact area by the substrate grids retained high specific pY levels (Fig. 3D). This effect was restricted to the periphery, because TCR clusters trapped in more central regions of spatially modified synapses lost their pY signal in a time frame similar to those observed in native synapses. The duration of TCR-pY signaling thus correlated with radial position of the TCR rather than with cluster size. Overall, the extent of specific pY associated with TCR clusters above the local background was significantly greater in the IS that had been spatially constrained by the grid (Fig. 3E).

Another key measure of signaling activity is the flux of intracellular Ca^{2+} induced by TCR antigen recognition, which integrates the outputs of all TCR signaling events in the IS (*18*). The integrated Ca^{2+} response was significantly higher in cells with spatially constrained IS as compared with those with native synapses (Fig. 3F). Thus, mechanical trapping of TCR in the IS periphery augments early TCR-associated pY levels, as well as the elevation of cytoplasmic Ca^{2+}.

These experiments provide insight into how signaling is extinguished in individual TCR clusters in the IS, which may be attributed to temporal or spatial processes such as recruitment of inhibitors (*19*) or changes in the actin cytoskeleton that feed back on signaling (*20*). The hybrid live cell–supported membrane platform made it possible to physically impede receptor translocation to prevent c-SMAC formation, allowing us to resolve that radial location represents a critical parameter in the IS. In physiological terms, it is possible that some APCs may use their own cytoskeletons to restrict transport of pMHC or costimulatory molecules in a related manner. Impeding TCR cluster translocation to the c-SMAC might thus represent a means of augmenting T cell activation (*21*, *22*). Potentially, the ability to induce spatial modifications in model cell-cell interfaces could be useful in exploring spatial organization of membrane domains and proteins on the cell surface, receptor signaling activity, and cytoskeletal regulation processes.

References and Notes

1. B. P. Babbitt *et al.*, *Nature* **317**, 359 (1985).
2. D. M. Davis, M. L. Dustin, *Trends Immunol.* **25**, 323 (2004).
3. P. Friedl, J. Storim, *Trends Cell Biol.* **14**, 557 (2004).
4. V. Das *et al.*, *Immunol. Rev.* **189**, 123 (2002).
5. C. L. Fuller, V. L. Braciale, L. E. Samelson, *Immunol. Rev.* **191**, 220 (2003).
6. M. Dykstra, A. Cherukuri, H. W. Sohn, S. J. Tzeng, S. K. Pierce, *Annu. Rev. Immunol.* **21**, 457 (2003).
7. T. Harder, *Curr. Opin. Immunol.* **16**, 353 (2004).
8. R. Tavano *et al.*, *J. Immunol.* **173**, 5392 (2004).
9. K.-H. Lee *et al.*, *Science* **302**, 1218 (2003).
10. G. Campi, R. Varma, M. L. Dustin, *J. Exp. Med.* **202**, 1031 (2005).
11. E. Sackmann, *Science* **271**, 43 (1996).
12. J. T. Groves, M. L. Dustin, *J. Immunol. Methods* **278**, 19 (2003).
13. A. Grakoui *et al.*, *Science* **285**, 221 (1999).
14. J. T. Groves, N. Ulman, S. G. Boxer, *Science* **275**, 651 (1997).
15. B. L. Jackson, J. T. Groves, *J. Am. Chem. Soc.* **126**, 13878 (2004).
16. M. M. Davis *et al.*, *Annu. Rev. Biochem.* **72**, 717 (2003).
17. K. H. Lee *et al.*, *Science* **295**, 1539 (2002).
18. D. J. Irvine, M. A. Purbhoo, M. Krogsgaard, M. M. Davis, *Nature* **419**, 845 (2002).
19. P. Fischer *et al.*, *Biochem. J.* **378**, 449 (2004).
20. J. Xu *et al.*, *Cell* **114**, 201 (2003).
21. S. Y. Tseng, M. Lu, M. L. Dustin, *J. Immunol.*, in press.
22. M. M. Al-Alwan, G. Rowden, T. D. Lee, K. A. West, *J. Immunol.* **166**, 1452 (2001).

23. We thank A. L. DeMond and R. Varma for helpful discussions. Supported by Boehringer Ingelheim (G.C.) and NIH grant GM64900.

Supporting Online Material

www.sciencemag.org/cgi/content/full/310/5751/1191/DC1
Materials and Methods
SOM Text
Figs. S1 to S4

23 August 2005; accepted 24 October 2005
10.1126/science.1119238

Regulation of Yeast Replicative Life Span by TOR and Sch9 in Response to Nutrients

Matt Kaeberlein,[1]* R. Wilson Powers III,[1] Kristan K. Steffen,[2] Eric A. Westman,[2] Di Hu,[2] Nick Dang,[2] Emily O. Kerr,[2] Kathryn T. Kirkland,[2] Stanley Fields,[1,3] Brian K. Kennedy[2]*

Calorie restriction increases life span in many organisms, including the budding yeast *Saccharomyces cerevisiae*. From a large-scale analysis of 564 single-gene–deletion strains of yeast, we identified 10 gene deletions that increase replicative life span. Six of these correspond to genes encoding components of the nutrient-responsive TOR and Sch9 pathways. Calorie restriction of *tor1Δ* or *sch9Δ* cells failed to further increase life span and, like calorie restriction, deletion of either *SCH9* or *TOR1* increased life span independent of the Sir2 histone deacetylase. We propose that the TOR and Sch9 kinases define a primary conduit through which excess nutrient intake limits longevity in yeast.

Calorie restriction (CR) is the only intervention known to increase life span in yeast, worms, flies, and mammals, but the molecular mechanism for this phenomenon has not been clear. In yeast, CR due to reduced glucose concentration of the culture medium increases replicative life span (the number of daughter cells produced by a given mother cell before senescence) by 20 to 40% (*1*–*3*). This increased life span has been attributed to activation of Sir2 (*1*), a histone deacetylase that is dependent on NAD (the oxidized form of nicotinamide adenine dinucleotide) (*4*) and that promotes longevity by inhibiting the formation of extrachromosomal ribosomal DNA (rDNA) circles (ERCs) in the nucleolus (*5*). Recently, however, the link between Sir2 and CR has been called into question with the discovery that Sir2 is not required for life-span extension by CR (*3*).

To identify genes that regulate longevity in the budding yeast, a large-scale analysis of replicative life span was conducted with the *MATα* haploid open reading frame (ORF) deletion collection, a set of ~4800 single-gene–deletion strains (*6*). Because replicative life-span analysis requires labor-intensive micromanipulation of daughter cells from mother cells, fewer than 80 different genes have been previously examined for their effect on replicative life span (*7*). Here we examined the replicative aging properties of 564 single-gene–deletion strains (Fig. 1A; table S1).

An iterative method was designed to identify ~95% of strains with mean replicative life span at least 30% longer than wild type (*8*). For each single-gene–deletion strain, replicative life span was initially determined for five individual mother cells. If the mean life span was less than 26 generations, the strain was classified as not-long-lived (NLL). This lower cutoff value is predicted to result in misclassification of a long-lived strain less than 5% of the time (fig. S1). If the mean life span was less than 20, the strain was classified as short-lived (SL). If the mean life span was greater than 36, the strain was putatively classified as long-lived (LL),

[1]Departments of Genome Sciences and Medicine, [2]Department of Biochemistry, University of Washington, Seattle, WA 98195, USA. [3]Howard Hughes Medical Institute, University of Washington, Seattle, WA 98195 USA.

*To whom correspondence should be addressed. E-mail: kaeber@u.washington.edu (M.K.); bkenn@u.washington.edu (B.K.K.)

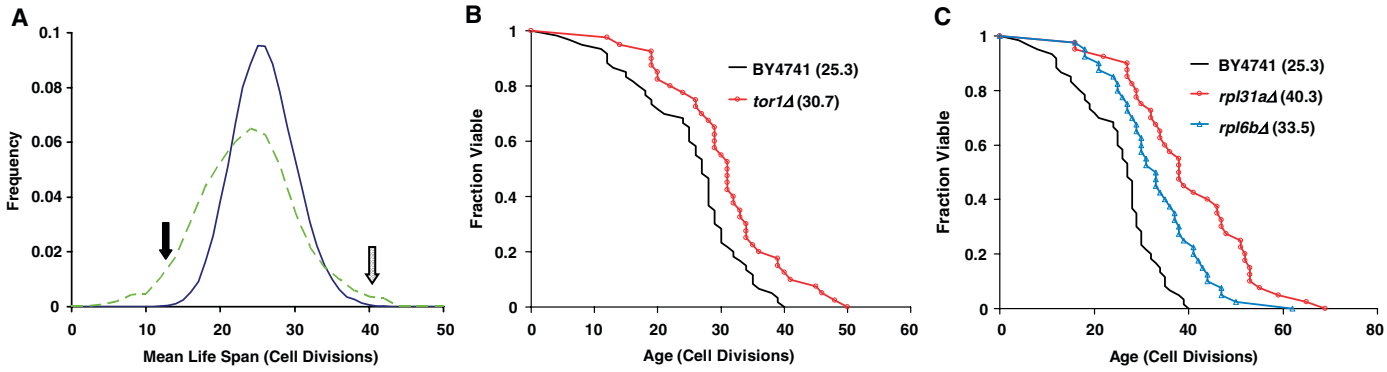

Fig. 1. TOR activity is an important modifier of yeast longevity. (**A**) The distribution of observed strain mean life spans for 564 single-gene–deletion mutants (broken line) shows an overrepresentation of short-lived (dark arrow) and long-lived (light arrow) mutants relative to expected mean life-span distribution (solid lines) for wild-type cells of the same sample size (n = 5). (**B**) Deletion of *TOR1* increases life span. (**C**) Deletion of either *RPL31A* or *RPL6B*, ribosomal proteins transcriptionally regulated by TOR, increases life span. Mean life spans are shown in parentheses.

and an additional 10 cells were examined. This upper cutoff value is predicted to result in misclassification of a strain with wild-type life span less than 2% of the time. For the remaining strains with a five-cell mean life span between 26 and 36 generations, an additional five cells were analyzed (one iteration), and the same classification scheme was applied. This process was repeated until every strain was either classified as SL, NLL, or LL or until replicative life span had been determined for a minimum of 15 cells for each unclassified strain. The replicative life-span data for strains from which at least 15 mother cells had been assayed were compared with cell life-span data from wild-type mothers, matched by experiment, by using a Wilcoxon rank-sum test to generate a P value. Strains with $P \leq 0.1$ were classified as LL, and strains with $P > 0.1$ were classified as having a life span not significantly extended (NSE). Of the 564 strains analyzed, 114 were classified as SL, 254 as NLL, 152 as NSE, and 44 as LL. Although nearly 20% of the gene deletions resulted in a significantly shortened life span, relatively few of these are likely to represent a true premature aging phenotype, because dysregulation of many different cellular processes will decrease fitness and longevity (*9*). For this reason, we focused on genes that, when deleted, resulted in increased replicative life span, reasoning that the proteins encoded by these genes must impede the normal aging process.

Of the 44 single-gene–deletion strains initially classified as LL, 13 result in a significant increase in replicative life span (Table 1). Verification was accomplished by determining the replicative life span for the corresponding gene deletion strain from the haploid *MAT***a** deletion collection and, in select cases, by generating a new deletion allele in the parental BY4742 strain. Of the 13 genes, *FOB1* served as a proof of principle that our method can identify a true-positive aging gene, because deletion of *FOB1* is known to increase life span by reducing the formation of ERCs (*10*). In two cases, gene deletions conferring increased life span occurred in overlapping ORFs encoded on opposite strands (*REI1* contains *YBR266C*; *IDH2* overlaps *YOR135C*), and longevity was comparable for overlapping deletion pairs (table S2). The identification of two different overlapping gene pairs from this screen suggests that a high fraction of true-positive genes were successfully identified.

The most striking feature of the 10 (excluding the overlapping dubious ORFs and *FOB1*) newly identified aging genes is that 6 are implicated in the TOR signaling pathway. TOR proteins are highly conserved from yeast to humans and regulate multiple cellular processes in response to nutrients, including cell size, autophagy, ribosome biogenesis and translation, carbohydrate and amino acid metabolism, stress response, and actin organization (*11*). Yeast has two TOR proteins, Tor1 and Tor2. Tor2 is essential and, therefore, not represented in the deletion collection. Deletion of *TOR1* was identified from this screen and found to increase both mean and maximum life span by ~20% (Fig. 1B). Two downstream targets of Tor1 and Tor2 were also identified: Ure2, which regulates activity of the nitrogen-responsive transcription factor Gln3, and Rom2, a proposed activator of protein kinase C (*12*, *13*). Deletion of three genes that are transcriptionally up-regulated by TOR increased life span: *YBR238C*, a gene of unknown function (*14*), and *RPL31A* and *RPL6B*, encoding two components of the large ribosomal subunit (Fig. 1C). Not all TOR-regulated ribosomal protein gene deletions examined conferred increased life span. Unlike the case in most multicellular eukaryotes, many of the ribosomal protein genes are duplicated in yeast (e.g., *RPL31A* and *RPL31B*), which allows for viable deletion of either paralog (but not both simultaneously). The relative importance of each paralog for ribosomal function, perhaps reflecting differential expression levels, may determine the longevity phenotype on deletion, with the gene coding for the more abundant member of the pair more likely to influence life span. Consistent with this idea, *rpl31aΔ* mother cells are long-lived and slow growing, whereas *rpl31bΔ* mother cells are not (fig. S2).

Table 1. Long-lived deletion strains. From a screen of 564 single-gene–deletion strains, 13 genes were found to increase replicative life span when deleted. GDP, guanosine diphosphate; GTP, guanosine 5′-triphosphate; PI3-like kinase, a kinase like phosphatidylinositol 3-kinase.

Deletion strain	Protein function
bre5Δ	Ubiquitin protease
fob1Δ	rDNA replication fork barrier protein
idh2Δ	Isocitrate dehydrogenase
rei1Δ	Protein of unknown function with similarity to human ZPR9
rom2Δ	GDP-GTP exchange factor for Rho1p
rpl31aΔ	Ribosomal protein L31
rpl6bΔ	Ribosomal protein L6
tor1Δ	PI3-like kinase involved in regulation of cell growth
ure2Δ	Regulator of nitrogen catabolite repression
ybr238cΔ	Protein of unknown function
ybr255wΔ	Protein of unknown function
ybr266cΔ	Hypothetical ORF overlapping *REI1*
yor135cΔ	Hypothetical ORF overlapping *IDH2*

Protein kinase A (PKA) and Sch9 are nutrient-responsive protein kinases that modulate replicative aging in yeast (*1*, *15*). Mutations that decrease PKA activity increase replicative life span and have been suggested as genetic models of CR (*1*, *3*). TOR is thought to act both upstream and parallel to PKA, whereas Sch9 is thought to act in a pathway parallel to PKA and TOR (*16*, *17*). TOR, PKA, and Sch9 regulate the expression of common downstream targets, including ribosomal proteins, such as Rpl31a and Rpl6b (*18*, *19*). CR of *tor1Δ* or *sch9Δ* cells failed to significantly increase the life span of these long-lived mutants (Fig. 2, A and B), which indicates that, similar to PKA, Sch9 and TOR are targets of CR in yeast. CR by growth

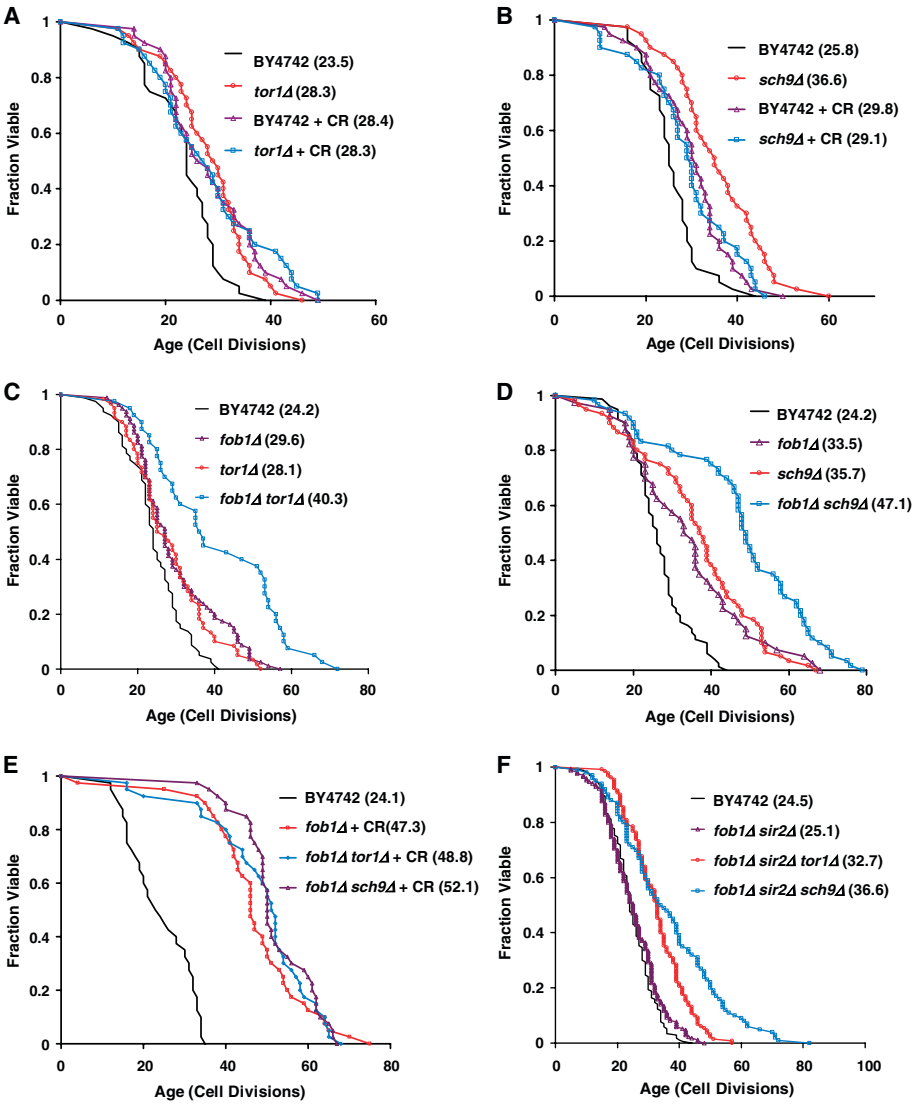

Fig. 2. *TOR1* or *SCH9* deletion mutants are genetic mimics of CR. (**A**) CR fails to further increase the life span of cells lacking *TOR1*. (**B**) CR fails to further increase the life span of cells lacking *SCH9*. (**C**) Deletion of *TOR1* increases life span additively with deletion of *FOB1*. (**D**) Deletion of *SCH9* increases life span additively with deletion of *FOB1*. (**E**) Deletion of either *TOR1* or *SCH9* fails to increase the life span of calorie-restricted *fob1Δ* cells. (**F**) Deletion of either *TOR1* or *SCH9* increases the life span of *sir2Δ fob1Δ* double-mutant cells. Mean life spans are shown in parentheses.

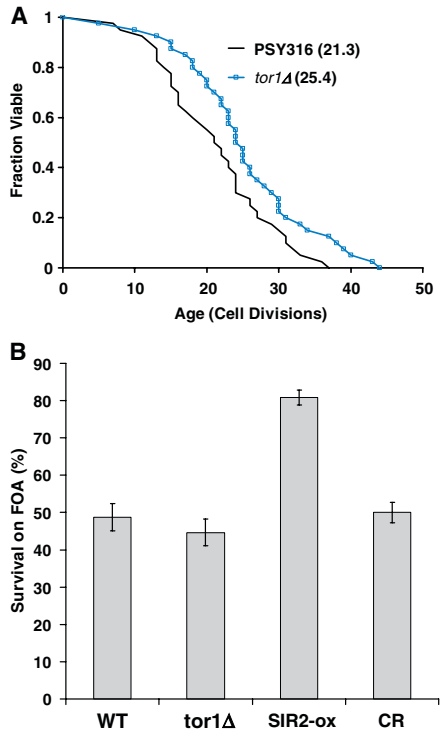

Fig. 3. Decreased TOR activity, like CR, is a strain-independent modifier of replicative life span. (**A**) Deletion of *TOR1* increases life span in the PSY316 background. Mean life spans are shown in parentheses. (**B**) Deletion of *TOR1* and CR have no effect on Sir2-dependent silencing of a telomeric *URA3* marker gene, as measured by survival in the presence of 5-FOA, in the PSY316 background. An extra copy of Sir2 (SIR2-ox) increases silencing of telomeric *URA3*. WT is wild-type.

on low glucose, or mutations resulting in decreased PKA activity, increase life span additively with deletion of *FOB1* (*3*). Deletion of *TOR1* or deletion of *SCH9* also resulted in an additive increase in life span when combined with deletion of *FOB1* (Fig. 2, C and D). The already long life span of the *sch9Δ fob1Δ* or *tor1Δ fob1Δ* mother cells was not further increased by CR (Fig. 2E). Life-span extension by CR also occurs independently of Sir2, as long as ERC formation is kept low through deletion of *FOB1* (*3*). Deletion of either *TOR1* or *SCH9* also increased the life span of *sir2Δ fob1Δ* cells (Fig. 2F). These epistasis experiments suggest that decreased activity of the nutrient-responsive kinases Sch9 and TOR in response to CR results in increased replicative life span in yeast.

Life-span extension by CR in yeast was initially characterized in the short-lived strain background PSY316 (*1*). PSY316 is unique among yeast strains used for longevity studies in that, although CR increases life span by 30 to 40%, deletion of *FOB1* or overexpression of *SIR2* fails to result in increased life span (*20*). To determine whether TOR activity is a general or strain-specific determinant of replicative life span, we examined the effect of *TOR1* deletion on life span and Sir2 activity in the PSY316 background. Deletion of *TOR1* significantly increased life span in PSY316, but had no effect on Sir2-dependent silencing at telomeres, similar to the effect of CR by growth on low glucose (Fig. 3, A and B). Thus, like CR, decreased TOR activity is a strain-independent mechanism to achieve enhanced longevity in yeast.

TOR activity is a primary determinant of replicative aging in yeast, and genetic analysis indicates that Sir2-independent life-span extension by CR is mediated by reduced signaling through TOR, Sch9, and PKA, resulting in down-regulation of ribosome biogenesis. Recently, an alternative model has suggested that Sir2-independent CR is caused by decreased ERC formation, resulting from nuclear relocalization and activation of the Sir2 homolog Hst2 (*21*). However, as long as ERC formation is maintained at a low level, CR increases life span to a greater extent in cells lacking Sir2 than in cells where Sir2 is present, seemingly inconsistent with Hst's simply playing a role redundant to Sir2's. CR increases life span additively with deletion of *FOB1*, which suggests a mechanism for CR that is independent of ERCs. ERCs also affect aging only in yeast, whereas the longevity-promoting role of CR has been evolutionarily conserved.

Decreased activity of TOR and Sch9 orthologs increases life span in *Caenorhabditis elegans* (*22*, *23*) and *Drosophila melanogaster* (*24*), as does mutation of the TOR-regulated S6 kinase (*24*), which promotes ribosomal protein maturation in multicellular eukaryotes. Therefore, the data presented here are consistent

with a model whereby CR increases life span through a highly conserved, Sir2-independent signaling network from nutrients to ribosomes.

References and Notes

1. S. J. Lin, P. A. Defossez, L. Guarente, *Science* **289**, 2126 (2000).
2. S. J. Lin *et al.*, *Nature* **418**, 344 (2002).
3. M. Kaeberlein, K. T. Kirkland, S. Fields, B. K. Kennedy, *PLoS Biol.* **2**, E296 (2004).
4. S. Imai, C. M. Armstrong, M. Kaeberlein, L. Guarente, *Nature* **403**, 795 (2000).
5. M. Kaeberlein, M. McVey, L. Guarente, *Genes Dev.* **13**, 2570 (1999).
6. E. A. Winzeler *et al.*, *Science* **285**, 901 (1999).
7. M. Kaeberlein, K. T. Kirkland, S. Fields, B. K. Kennedy, *Mech. Ageing Dev.* **126**, 491 (2005).
8. Materials and methods are available as supporting material on *Science* Online.
9. M. Kaeberlein, B. K. Kennedy, *Mech. Ageing Dev.* **126**, 17 (2005).
10. P. A. Defossez *et al.*, *Mol. Cell* **3**, 447 (1999).
11. T. Schmelzle, M. N. Hall, *Cell* **103**, 253 (2000).
12. T. Beck, M. N. Hall, *Nature* **402**, 689 (1999).
13. S. B. Helliwell, I. Howald, N. Barbet, M. N. Hall, *Genetics* **148**, 99 (1998).
14. A. F. Shamji, F. G. Kuruvilla, S. L. Schreiber, *Curr. Biol.* **10**, 1574 (2000).
15. P. Fabrizio, S. D. Pletcher, N. Minois, J. W. Vaupel, V. D. Longo, *FEBS Lett.* **557**, 136 (2004).
16. S. A. Zurita-Martinez, M. E. Cardenas, *Eukaryot. Cell* **4**, 63 (2005).
17. I. Pedruzzi *et al.*, *Mol. Cell* **12**, 1607 (2003).
18. P. Jorgensen *et al.*, *Genes Dev.* **18**, 2491 (2004).
19. D. E. Martin, A. Soulard, M. N. Hall, *Cell* **119**, 969 (2004).
20. M. Kaeberlein *et al.*, *J. Biol. Chem.* **280**, 17038 (2005).
21. D. W. Lamming *et al.*, *Science* **309**, 1861 (2005); published online 28 July 2005 (10.1126/science.1113611).
22. M. Hertweck, C. Gobel, R. Baumeister, *Dev. Cell* **6**, 577 (2004).
23. T. Vellai *et al.*, *Nature* **426**, 620 (2003).
24. P. Kapahi *et al.*, *Curr. Biol.* **14**, 885 (2004).

25. We thank G. Martin and P. Rabinovitch for advice and helpful discussion. M.K. is supported by NIH training grant P30 AG013280 and by the Ellison Medical Foundation. This work was funded by awards to B.K. from the University of Washington Nathan Shock Center of Excellence for the Basic Biology of Aging, the American Federation for Aging Research, and the Ellison Medical Foundation. S.F. is an investigator of the Howard Hughes Medical Institute. B.K. is a Searle scholar. M.K. cofounded and served as vice president, Biology of Aging Research for Longenity, Inc., until May 2003.

Supporting Online Material

www.sciencemag.org/cgi/content/full/310/5751/1193/DC1
Materials and Methods
Figs. S1 to S3
Tables S1 and S2
References and Notes

31 May 2005; accepted 5 October 2005
10.1126/science.1115535

Golgi Duplication in *Trypanosoma brucei* Requires Centrin2

Cynthia Y. He, Marc Pypaert, Graham Warren*

Centrins are highly conserved components of the centrosome, which in the parasitic protozoan *T. brucei* comprises the basal body and nucleates the flagellum used for locomotion. Here, we found TbCentrin2 in an additional bi-lobed structure near to the Golgi apparatus. One lobe was associated with the old Golgi, and the other became associated with the newly forming Golgi as the cell grew. Depletion of TbCentrin1 inhibited duplication of the basal body, whereas depletion of TbCentrin2 also inhibited duplication of the Golgi. Thus, a Centrin2-containing structure distinct from the basal body appears to mark the site for new Golgi assembly.

Organelle duplication helps to ensure propagation through successive generations. For the Golgi apparatus, a number of models have been put forward, which differ as to the role played by the old Golgi in the construction of the new (*1*). What has not been addressed is the mechanism that determines the location for assembly of the new Golgi. In the budding yeast, *Pichia pastoris*, this location appears to be random, based on the probability of components reaching a critical mass for assembly (*2*). In several parasitic protozoa and in other protists, however, this location seems to be defined (*1*, *3*). In *T. brucei*, for example, there is a single Golgi, and a new copy is assembled at a fixed distance away (*4*). This new assembly site is somehow related to the new basal body (*5*); inhibition of basal-body segregation inhibits that of the Golgi (*4*) and inhibits division of the replicated kinetoplast, which contains all of the mitochondrial DNA (*6*). Basal bodies in particular and centrosomes in general have been implicated in the biogenesis of a number of membrane-bound organelles, in a variety of organisms (*6*, *7*), prompting us to study further their role in Golgi duplication.

Centrins are Ca^{2+}-binding proteins that are highly conserved and essential components of all centrosomes (*8*). The monoclonal antibody, 20H5, raised against *Chlamydomonas reinhardtii* Centrin (*9*), labels centrosomes in a wide range of organisms. It can also stain the basal bodies in *T. brucei* at different stages of the cell cycle (Fig. 1). The basal bodies are closely associated with the kinetoplast and mediate the division of the replicated kinetoplast (*6*).

The 20H5 antibody stained an additional, bi-lobed structure (Fig. 1). Early in the cell cycle, the old Golgi was adjacent to one lobe (Fig. 1A), whereas the new Golgi was later seen to be adjacent to the other, more posterior lobe (Fig. 1B), suggesting that it might be marking the site for new assembly. As the new Golgi grew and increasingly separated from the old (Fig. 1C), the bi-lobed structure itself duplicated, so that one remained with the old Golgi and one with the new (Fig. 1, D and E). This occurred at about the same time as the division of the replicated kinetoplast (Fig. 1E).

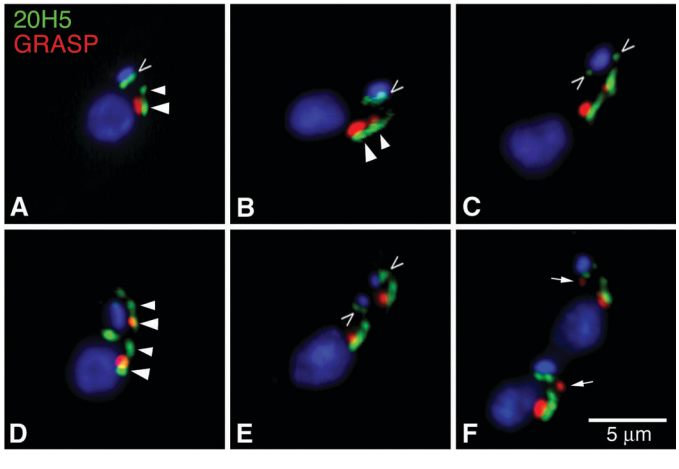

Fig. 1. A Centrin-containing structure associated with the Golgi. Gallery of images through the cell cycle of cells triple labeled for Golgi [anti–Golgi Reassembly Stacking Protein (GRASP), red], Centrin (20H5, green), and DNA [4′,6′-diamidino-2-phenylindole (DAPI), blue]. Basal bodies [open arrowheads (**A** and **B**)] underwent duplication (**C** and **D**) and mediated the division of the replicated kinetoplast (**E**). Centrin associated with the Golgi was present in a bi-lobed structure (solid arrowheads), with one lobe near to the old Golgi (A) and the other more toward the posterior of the parasite, marking the site where the new Golgi was undergoing assembly [compare (A) and (B)]. Increasing separation of the old and new Golgi (C) was accompanied by duplication of this bi-lobed structure [(C) to (E)] at about the same time as the replicated kinetoplast divided (E). (**F**) Just before cytokinesis, additional Golgi (arrows) appeared that were not associated with Centrin. Scale bar, 5 μm.

Department of Cell Biology, Yale University School of Medicine, 333 Cedar Street, New Haven, CT 06520, USA.

*To whom correspondence should be addressed. E-mail: graham.warren@yale.edu

www.sciencemag.org/cgi/content/full/310/5751/1193/DC1

Supporting Online Material for

Regulation of Yeast Replicative Life Span by TOR and Sch9 in Response to Nutrients

Matt Kaeberlein,* R. Wilson Powers III, Kristan K. Steffen, Eric A. Westman, Di Hu, Nick Dang, Emily O. Kerr, Kathryn T. Kirkland, Stanley Fields, Brian K. Kennedy*

*To whom correspondence should be addressed. Departments of Genome Sciences and Medicine (M.K.), Department of Biochemistry (B.K.K.), University of Washington, Seattle, WA 98195, USA. E-mail: kaeber@u.washington.edu (M.K.); bkenn@u.washington.edu (B.K.K.)

Published 18 November 2005, *Science* **310**, 1193 (2005)
DOI: 10.1126/science.1115535

This PDF file includes

SUPPORTING ONLINE MATERIAL

Materials and Methods

Strains and Media

Unless otherwise stated, all yeast strains were derived from the parent strains for the haploid yeast ORF deletion collections (*S1*), BY4742 *MATαhis3Δ1 leu2Δ0 lys2Δ0 ura3Δ0* and BY4741 *MAT*a *his3Δ1 leu2Δ0 met15Δ0 ura3Δ0*. The *MAT*α haploid ORF deletion collection and the *MAT*a haploid ORF deletion collection, along with the parental strains, were obtained from Research Genetics. PSY316AUT containing telomeric *ADE2* and *URA3* markers used for determination of telomere silencing in Figure 3 was derived from PSY316 *MAT*α *ura3-52 leu2*-3,*112 his3- 200 ade2-101 lys2801*, and is as described (*S2*). Gene disruptions were carried out by transforming yeast with PCR-amplified deletion constructs containing 45 nucleotides of homology to regions flanking the ORF to be deleted and either *HIS3*, *LEU2*, or *URA3* amplified from pRS403, pRS405, or pRS406 (*S3*), respectively. In each case, the entire open reading frame of the deleted gene was removed. All gene disruptions were verified by PCR. Methionine sulfoximine (MSX) was obtained from Sigma, dissolved in water at a concentration of 50 mM, and stored at 4°C.

Genome-wide screen for single-gene deletions with increased replicative life span

Four different genome-wide deletion collections are available (Open Biosystems) that would, in principle, be suitable for a replicative life-span study of the type described here: haploid mating type α (*MAT*α), haploid mating type a (*MAT*a), homozygous diploid, and heterozygous diploid. In choosing which collection to assay for replicative life span, we immediately excluded the heterozygous diploid deletion collection, since the majority of genes affecting yeast aging are unlikely to be haploinsufficient. From the remaining collections, we chose to utilize the haploid *MAT*α collection for several reasons. First, the vast majority of prior studies on yeast aging have been carried out in haploid strains, making data obtained from this analysis more directly comparable to previous work. Second, we had already generated a large data set containing replicative life-span information on several dozen deletion strains from the haploid *MAT*α collection (*S4*), including greater than 500 mother cell life spans for wild type and 500 mother cell life spans for long-lived mutants. This data was used to develop the iterative screening method described below. Third, performing the initial screen in the haploid *MAT*α collection allowed us to use the *MAT*a haploid collection to verify putative long-lived deletion mutants (see below). The presence of aneuploidy and other genetic anomalies in about 10% of strains derived from the deletion collection has also been reported (*S5*), making verification of long-lived mutants essential. One potential disadvantage of using a haploid collection, as opposed to the diploid collection, is the possibility that spontaneous recessive mutations could arise which alter the replicative life span of the deletion strain being tested. This may account for some portion of the strains that failed to pass the verification step.

To establish replicative life-span data for the entire yeast deletion set is a daunting task that precludes the possibility of analyzing a large number of cells from each deletion strain. We have used statistical approaches based on data generated in the BY4742 strain

background to determine a minimal number of cells analyzed per strain necessary for (i) a semi-quantitative determination of mean replicative life span and (ii) isolation of at least 95% of the gene deletions which result in at least a 30% extension of mean life span. This approach will also lead to the identification of a number of gene deletions that result in life-span extension that is statistically significant ($p < 0.05$, Wilcoxon rank-sum test) but less than a 30% extension. We have previously reported a large-scale systematic analysis of known aging genes in the BY4742 background (*S4*), including a number of gene deletions that extend mean replicative life span by approximately 30%. This analysis entailed determining the replicative life spans for greater than 10,000 mother cells, of which more than 500 were wild type (BY4742) and more than 500 were from strains with a mean replicative life span at least 30% greater than BY4742 (*hxk2*Δ, *gpa2*Δ, *gpr1*Δ, and *fob1*Δ). This data was used as a starting point for designing an iterative process for genome-wide replicative life-span analysis.

The replicative life-span data for wild-type ($N > 500$) was compiled into one set (WT) and replicative life-span data for the known long-lived mutants *hxk2*Δ, *gpa2*Δ, *gpr1*Δ, and *fob1*Δ ($N > 500$) was compiled into a second set (LLM). Probability distributions were then generated for mean life span as a function of the number of cells examined (n), when n = 3, 5, 10, 15, and 20 for WT and LLM, respectively (e.g. Fig. 1 shows the theoretical distributions for WT n = 5). For example, the n = 3 distribution for wild-type was generated by randomly choosing 3 data points from the pooled wild-type life-span set, calculating the mean of the 3 values, and repeating the process 100,000 times. A histogram was then generated for the probability that a particular mean life span is obtained for a set size n = 3, with bins of width 0.1 generation.

From this numerical analysis, we were able to establish that an iterative strategy, initially analyzing the replicative life span of 5 cells per deletion strain, should allow us to identify a large fraction of the strains with a mean life span greater than 30% longer than wild type (Fig. S1). For each mutant, based on n = 5 mother cells, if the mean life span was less than 26, the strain was classified as not long-lived (NLL). From the cumulative probability distribution for known long-lived strains, n = 5, this is predicted to result in misclassification of a long-lived strain less than 5% of the time (false negative rate, $FNR < 0.05$). If the mean life span was less than 20, the strain was classified as short-lived (SL), and a p-value was assigned based on the cumulative probability distribution for wild-type cells, n = 5. If the mean life span for 5 cells was greater than 36, the strain was putatively classified as long-lived (LL) and an additional 10 cells were examined. From the cumulative probability distribution for wild-type cells, n = 5, this is predicted to result in misclassification of a strain with wild-type life span less than 2% of the time (false positive rate, $FPR < 0.02$). For the remaining strains with a 5-cell mean life span between 26 and 36, an additional 5 cells were analyzed (1 iteration) and the same criteria for classification were applied. This process was repeated until every strain was either classified as SL, NLL, or LL, or until replicative life span had been determined for a total of at least 15 cells for each unclassified strain. The replicative life-span data for strains from which at least 15 mother cells had been assayed was compared against experiment-matched wild-type replicative life-span data using a Wilcoxon Rank-Sum test and a p-value was generated. Strains with $p \leq 0.1$ were classified as LL, and strains with $p > 0.1$ were classified as having no significant life-span extension (NSE).

In practice, replicative life-span analysis the deletion set was carried out in 95-strain sets (94 deletion strains and wild-type). The ORF deletion collection is packaged in 96-well plates, each plate containing 94 strains. Life span was determined for 5 cells per strain, with 12 strains (one row of the 96-well plate) analyzed per 100 mm YPD plate. Each 96well plate was chosen randomly from the deletion set, with the exception of the first plate analyzed, which was chosen because it contained our true-positive control, *fob1*Δ. The plate numbers examined, in chronological order, were #110, #135, #118, #128, #149, and #114. In addition to the strains contained on the 6 plates, we carried out replicative life-span analysis on three additional strains, *ure2*Δ, *gat1*Δ, and *gln3*Δ, which were included in the analysis. Mean life-span data for each of the 564 strains, along with experiment-matched wild-type life-span data, is provided (Table S1).

From this analysis, 44 deletion strains were classified as LL (Table S2). Given the expected FPR, along with documented reports of aneuploidy, diploidization, and other anomalies in the deletion set, we next performed a series of verification steps to determine which of these 44 deletions strains were indeed long-lived. Thus far, 13 strains have been verified as long-lived (Table 1). Verification was accomplished by first determining the replicative life span for strains corresponding to each gene deletion mutant obtained from the *MAT*a ORF deletion collection. Replicative life span was determined for a minimum of 40 cells from each mutant (Table S2). In select cases, a new deletion allele was generated in the parental BY4742 strain, and life span was determined.

Life-span extension by chemical inhibition of TOR

Chemical inhibitors of Tor1 and Tor2 have been described, allowing us to assess life-span effects caused by pharmacological down-regulation of TOR activity. One chemical inhibitor of TOR activity that is suitable for replicative life-span assays is methionine sulfoximine (MSX), an inhibitor of glutamine synthetase. TOR activity in yeast is regulated by intracellular glutamine levels, and treatment of cells with MSX has been shown to inhibit both Tor1 and Tor2 by decreasing intracellular glutamine (S6). Addition of MSX to the media resulted in a dose-dependent increase in mean and maximum life span, up to a concentration of 2.5 mM (Fig. S3). Concentrations of 100μM and 1 mM MSX led to a statistically significant increase in both mean and maximum life span ($p < 0.05$), comparable to that observed upon deletion of TOR1. Thus, reducing TOR activity slows aging in yeast, and treatment with a TOR inhibitor increases life span.

Replicative life-span analysis

Strains from the yeast ORF deletion collection were prepared for replicative life-span analysis by transferring a small volume (~1 μL) from frozen stock onto YPD agar using a Biomek FX robot equipped with an HDR 96-pin tool. Each strain was allowed to grow overnight at 30°C and then a small number of cells was patched onto a fresh YPD plate used for life-span analysis. Otherwise, yeast strains for replicative life-span analysis were removed from frozen stock (25% glycerol, -80°C) individually and streaked onto YPD. After 2 days growth, single colonies were selected and patched to YPD. The next evening, cells were lightly patched to the plates used for life-span analysis.

After overnight growth on the life-span plates, cells were arrayed on the YPD plate using a micromanipulator and allowed to undergo 1-2 divisions. Virgin cells were then

selected and subjected to life-span analysis. Plates were sealed with Parafilm, except during dissection. Cells were grown at 30°C during the day and stored at 4°C at night. Daughter cells were removed by gentle agitation with a dissecting needle and tabulated every 2-4 hours. All life-span experiments were carried out on standard YPD plates (2% glucose, unless otherwise noted). In order to prevent possible bias, strains were coded such that the researcher performing the life-span experiment had no knowledge of the strain genotype for any particular strain. For each experiment, each strain was randomly assigned a numerical identifier at the time of removal from frozen stock. One individual was responsible for assigning strain designations while a different individual performed the replicative life-span analysis. For statistical analysis, life-span datasets were compared by a two-tailed Wilcoxon Rank-Sum test. Wilcoxon p-values were calculated using the MATLAB 'ranksum' function.

For life-span studies with MSX, the drug was added from frozen stock to melted and cooled YPD at the indicated concentration. Cells were grown on YPD + MSX media overnight prior to micromanipulation and life-span determination.

FOA telomere silencing assays

Transcriptional silencing of the telomeric *URA3* marker in PSY316AUT was determined by survival on media supplemented with 5-fluoroorotic acid (FOA), which is toxic to cells expressing *URA3*. Cells were cultured in liquid YPD or YEP + 0.05% glucose (CR media) overnight. The next morning, each overnight culture was diluted 1:100 into YPD or YEP + 0.05% glucose (CR media) and grown for 4 hours in a shaking incubator. Cultures were then diluted to a cell density of approximately 2×10^3 cells/mL in water, and plated in 100 µL aliquots onto synthetic complete (SC) or FOA media containing either 2% or 0.05% glucose (CR), as noted. Percent survival was calculated as the number of colonies arising on FOA media divided by the number of colonies arising on SC media.

References

S1. E. A. Winzeler *et al.*, *Science* **285**, 901-6 (Aug 6, 1999).
S2. M. Kaeberlein *et al.*, *J Biol Chem* **280**, 17038-45 (Apr 29, 2005).
S3. R. S. Sikorski, P. Hieter, *Genetics* **122**, 19-27 (May, 1989).
S4. M. Kaeberlein, K. T. Kirkland, S. Fields, B. K. Kennedy, *Mech Ageing Dev* **126**, 491-504 (Apr, 2005).
S5. T. R. Hughes *et al.*, *Nat Genet* **25**, 333-7 (Jul, 2000).
S6. J. L. Crespo, T. Powers, B. Fowler, M. N. Hall, *Proc Natl Acad Sci U S A* **99**, 6784-9 (May 14, 2002).

Supplemental Table 1. Replicative life span data for 564 strains contained in the *MATα* yeast ORF deletion collection. For each strain examined the mean life span of the gene deletion mutant (Deletion Mean) and the number of mutant cells examined (Deletion N) is shown along with the mean life span (WT Mean) and number (WT N) of wild-type BY4742 cells contained in the same experiment. Strains were classified (Class) according to the criteria described in the supplemental methods. *Wilcoxon Rank-Sum test p-value < 0.05. **Wilcoxon Rank-Sum test p-value < 0.01.

ORF	Gene	Class	Deletion Mean	Deletion N	WT Mean	WT N
YAL012W	CYS3	NSE	30.2	25	24.5	25
YAL024C	LTE1	NLL	25.8	10	27.0	10
YAL047C	SPC72	SL**	4.0	5	28.8	5
YAL054C	ACS1	NLL	24.5	10	26.1	10
YAL056C-A		NLL	23.6	5	28.8	5
YAR050W	FLO1	NLL	21.0	5	28.8	5
YBR223C	TDP1	NLL	22.4	10	29.6	10
YBR224W		NLL	24.3	10	29.6	10
YBR225W		SL*	17.6	10	29.6	10
YBR226C		NSE	31.8	20	29.6	20
YBR227C	MCX1	NLL	20.0	10	29.6	10
YBR228W	SLX1	NSE	26.3	15	25.2	20
YBR229C	ROT2	NLL	23.1	10	29.6	10
YBR230C		NLL	21.4	10	29.6	10
YBR231C	AOR1	SL**	15.9	10	29.6	10
YBR233W	PBP2	NLL	24.0	10	29.6	10
YBR235W		NLL	24.3	10	29.6	10
YBR238C		LL*	34.9	20	27.9	20
YBR239C		NLL	24.1	10	29.6	10
YBR240C	THI2	NSE	32.5	30	28.4	30
YBR241C		NLL	23.8	10	29.6	10
YBR242W		NSE	27.7	25	26.6	30
YBR244W	GPX2	SL*	19.5	10	29.6	10
YBR245C	ISW1	SL*	18.8	10	29.6	10
YBR246W		NLL	25.0	10	29.6	10
YBR248C	HIS7	NLL	24.9	10	29.6	10
YBR249C	ARO4	NSE	26.5	15	28.5	15
YBR250W		NLL	25.5	10	29.6	10
YBR255W		LL**	34.1	20	25.5	50
YBR258C	SHG1	SL*	22.5	10	29.6	10
YBR259W		NSE	27.1	30	28.4	30
YBR260C	RGD1	NLL	24.6	10	29.6	10
YBR261C		NSE	33.1	20	27.9	20
YBR262C	FMP51	SL**	17.3	10	29.6	10
YBR263W	SHM1	NSE	28.5	15	28.5	15
YBR264C	YPT10	NLL	23.0	10	29.6	10
YBR266C		LL**	37.3	80	27.3	80
YBR267W		LL**	37.5	50	27.3	50
YBR299W	MAL32	NLL	24.6	5	28.2	5
YCL006C		NSE	29.5	20	24.8	50
YCL022C		NLL	22.0	5	28.8	5

YCL023C		NLL	24.0	5	28.8	5
YCL038C	ATG22	NLL	24.6	5	28.8	5
YCL058C	FYV5	NLL	21.0	5	28.8	5
YCL074W		SL	17.8	5	28.8	5
YCL075W		NSE	28.5	20	26.3	20
YCL076W		NLL	23.0	5	28.8	5
YCR107W	AAD3	NSE	27.9	15	25.9	15
YDL047W	SIT4	NSE	30.8	15	26.8	20
YDL061C		NLL	25.0	5	28.2	5
YDL075W	RPL31A	LL**	32.5	30	25.4	40
YDR049W		SL*	22.4	10	29.6	10
YDR051C		NLL	22.1	10	29.6	10
YDR055W	PST1	NLL	25.3	15	28.5	15
YDR056C		NSE	28.7	20	26.9	30
YDR057W	YOS9	SL**	16.2	10	29.6	10
YDR059C	UBC5	NLL	22.2	10	29.6	10
YDR061W		NLL	25.1	10	29.6	10
YDR063W		NLL	23.8	10	29.6	10
YDR065W		SL**	15.6	10	29.6	10
YDR066C		NSE	27.5	15	28.5	15
YDR067C		NLL	25.6	10	29.6	10
YDR068W	DOS2	NSE	27.4	20	26.9	30
YDR069C	DOA4	SL**	15.8	10	29.6	10
YDR070C	FMP16	SL**	18.6	10	29.6	10
YDR072C	IPT1	SL*	20.6	10	29.6	10
YDR073W	SNF11	NSE	30.5	30	28.4	30
YDR075W	PPH3	SL*	23.8	10	29.6	10
YDR076W	RAD55	SL**	12.0	10	29.6	10
YDR078C	SHU2	NLL	24.8	10	29.6	10
YDR079W	PET100	NLL	25.2	10	29.6	10
YDR080W	VPS41	SL**	16.7	10	29.6	10
YDR083W	RRP8	NSE	31.1	20	28.1	20
YDR084C	TVP23	SL*	21.4	10	29.6	10
YDR085C	AFR1	NLL	23.4	10	29.6	10
YDR089W		SL*	20.8	10	29.6	10
YDR090C		SL*	24.7	15	28.5	15
YDR092W	UBC13	NLL	22.2	10	29.6	10
YDR093W	DNF2	NLL	22.9	15	25.2	20
YDR094W		NLL	23.6	10	29.6	10
YDR095C		SL**	20.1	10	29.6	10
YDR096W	GIS1	NLL	25.0	10	29.6	10
YDR097C	MSH6	NSE	30.7	20	26.2	30
YDR098C	GRX3	NSE	27.1	15	28.5	15
YDR099W	BMH2	NSE	26.1	15	28.5	15
YDR100W	TVP15	SL**	15.6	10	29.6	10
YDR101C	ARX1	NLL	26.0	15	28.5	15
YDR102C		NSE	26.7	20	29.6	20
YDR104C	SPO71	NSE	27.3	15	30.1	20
YDR105C	TMS1	NLL	23.9	10	29.6	10
YDR107C		NLL	24.7	10	29.6	10
YDR108W	GSG1	NLL	24.7	15	28.5	15
YDR109C		NLL	25.0	10	29.6	10

YDR110W	FOB1	LL**	32.1	40	26.6	40
YDR111C	ALT2	SL	19.7	10	29.6	10
YDR112W		SL*	20.9	10	29.6	10
YDR116C	MRPL1	NLL	23.5	10	29.6	10
YDR117C		NLL	23.2	10	29.6	10
YDR119W		NSE	29.4	25	29.9	30
YDR120C	TRM1	NLL	22.5	10	29.6	10
YDR121W	DPB4	NLL	25.9	10	29.6	10
YDR122W	KIN1	NLL	25.1	20	29.6	20
YDR123C	INO2	NLL	25.5	10	29.6	10
YDR124W		LL*	35.4	20	27.9	20
YDR125C	ECM18	NSE	26.2	20	29.6	20
YDR126W	SWF1	SL**	15.1	10	29.6	10
YDR128W		SL**	19.6	10	29.6	10
YDR129C	SAC6	SL**	10.5	20	29.6	20
YDR130C	FIN1	SL*	19.9	10	29.6	10
YDR131C		NLL	24.7	10	29.6	10
YDR132C		SL**	17.9	10	29.6	10
YDR133C		NLL	22.9	10	29.6	10
YDR134C		SL*	19.8	10	29.6	10
YDR242W	AMD2	NLL	24.6	20	26.6	20
YDR244W	PEX5	NSE	27.3	20	26.9	35
YDR245W	MNN10	NSE	32.5	20	25.9	55
YDR247W	VHS1	LL*	34.0	20	25.9	55
YDR248C		LL*	34.6	25	29.5	25
YDR249C		NLL	25.0	15	29.1	20
YDR250C		NSE	32.8	20	28.6	25
YDR251W	PAM1	NSE	29.9	20	26.9	35
YDR252W	BTT1	NLL	24.8	5	29.0	5
YDR253C	MET32	NSE	28.7	15	29.1	20
YDR254W	CHL4	NLL	22.6	10	27.4	10
YDR255C	RMD5	NSE	27.5	15	27.1	15
YDR256C	CTA1	NSE	29.9	20	26.9	35
YDR257C	RMS1	NLL	25.8	5	29.0	5
YDR258C	HSP78	NLL	25.2	10	27.4	10
YDR259C	YAP6	NLL	24.1	10	27.4	10
YDR260C	SWM1	NSE	31.1	20	26.9	35
YDR261C	EXG2	SL	19.8	5	29.0	5
YDR262W		NLL	21.4	5	29.0	5
YDR263C	DIN7	NLL	22.6	5	29.0	5
YDR264C	AKR1	SL**	7.2	5	29.0	5
YDR265W	PEX10	NLL	21.4	5	29.0	5
YDR266C		NSE	30.4	20	26.9	35
YDR268W	MSW1	NSE	36.1	15	29.4	15
YDR270W	CCC2	SL	17.8	5	29.0	5
YDR272W	GLO2	NLL	21.4	5	29.0	5
YDR273W	DON1	SL	19.8	5	29.0	5
YDR274C		LL	35.0	20	28.6	25
YDR275W	BSC2	NSE	32.1	15	27.3	15
YDR276C	PMP3	NSE	28.6	15	29.1	20
YDR277C	MTH1	NSE	28.7	20	28.6	25
YDR278C		NSE	34.1	15	29.4	15

YDR279W	RNH202	NLL	25.1	15	29.1	20
YDR281C	PHM6	NSE	29.7	20	26.9	35
YDR282C		SL	17.0	5	29.0	5
YDR283C	GCN2	NSE	30.6	15	27.3	15
YDR284C	DPP1	NSE	31.7	20	25.9	55
YDR285W	ZIP1	NLL	22.6	5	29.0	5
YDR286C		NSE	28.0	20	26.9	35
YDR287W		SL*	10.0	5	29.0	5
YDR289C	RTT103	NLL	24.3	15	29.1	20
YDR291W		SL	18.6	5	29.0	5
YDR293C	SSD1	NLL	24.8	5	29.0	5
YDR294C	DPL1	NLL	23.8	15	27.3	15
YDR295C	HDA2	NSE	31.9	20	26.9	35
YDR296W	MHR1	NLL	23.0	5	29.0	5
YDR297W	SUR2	NLL	23.0	5	29.0	5
YDR298C	ATP5	SL	16.8	5	29.0	5
YDR300C	PRO1	NSE	28.8	20	26.9	35
YDR304C	CPR5	NLL	25.6	5	29.0	5
YDR305C	HNT2	NLL	23.0	5	29.0	5
YDR306C		NSE	27.8	20	26.9	35
YDR307W		LL**	35.1	20	26.9	35
YDR309C	GIC2	NLL	24.0	5	29.0	5
YDR310C	SUM1	NLL	23.7	10	27.4	10
YDR312W	SSF2	NLL	22.3	10	27.4	10
YDR313C	PIB1	LL*	38.8	15	29.4	15
YDR314C		NSE	35.9	15	29.4	15
YDR315C	IPK1	LL**	36.6	20	25.9	55
YDR316W		SL	16.8	5	29.0	5
YDR317W		NSE	28.1	20	26.9	35
YDR318W	MCM21	NSE	28.8	20	26.9	35
YDR319C		NSE	30.7	20	26.9	35
YDR320C	SWA2	NSE	26.2	15	29.1	20
YDR321W	ASP1	NSE	31.5	20	26.9	35
YDR322W	MRPL35	NLL	22.4	5	29.0	5
YDR323C	PEP7	NLL	24.5	10	27.4	10
YDR326C		NSE	31.3	15	26.2	20
YDR329C	PEX3	NLL	22.8	5	29.0	5
YDR330W		NLL	25.4	5	29.0	5
YDR333C		SL	19.2	5	29.0	5
YDR334W		NSE	28.3	20	26.4	20
YDR335W	MSN5	NSE	29.1	15	29.4	15
YDR336W		NSE	29.2	15	27.3	15
YDR337W	MRPS28	NSE	34.3	15	29.4	15
YDR417C		NLL	23.5	10	27.0	10
YDR444W		SL	17.8	5	28.2	5
YDR461W	MFA1	NLL	25.3	15	26.7	15
YDR477W	SNF1	LL	36.5	15	26.8	15
YDR493W	FMP36	NLL	23.3	15	26.2	20
YDR500C	RPL37B	NSE	29.2	15	26.8	20
YDR502C	SAM2	NLL	23.2	10	27.0	10
YDR506C		NSE	28.7	15	26.2	20
YDR512C	EMI1	NLL	25.8	15	26.2	20

YDR515W	SLF1	NSE	26.6	15	26.7	15
YER040W	GLN3	SL*	20.4	40	24.4	40
YER089C	PTC2	NLL	24.7	10	27.0	10
YER170W	ADK2	NLL	23.6	5	28.2	5
YER173W	RAD24	NLL	21.6	5	28.2	5
YER174C	GRX4	NLL	25.6	5	28.2	5
YER175C	TMT1	NSE	27.4	20	25.0	30
YER176W	ECM32	NSE	30.8	15	26.2	20
YER177W	BMH1	NLL	21.8	5	28.2	5
YER178W	PDA1	SL*	12.4	5	28.2	5
YER179W	DMC1	NLL	26.0	10	27.0	10
YER180C	ISC10	NLL	22.2	10	27.0	10
YER181C		NSE	29.1	20	24.7	50
YER182W	FMP10	NLL	24.9	15	26.7	15
YER183C	FAU1	NSE	26.5	15	26.7	15
YER184C		NLL	24.6	5	28.2	5
YER185W		NSE	27.1	15	26.7	15
YER186C		LL*	31.3	20	24.7	50
YER187W		LL*	36.2	20	26.2	20
YFL001W	DEG1	NLL	23.6	10	27.0	10
YFL021W	GAT1	NSE	26.3	20	24.4	40
YGL199C		SL	17.2	5	28.8	5
YGL214W		NSE	29.7	15	26.3	20
YGL217C		NSE	26.8	15	26.3	20
YGL235W		NSE	30.7	15	26.3	20
YGR011W		NSE	29.0	15	26.3	20
YGR018C		NLL	20.8	5	28.8	5
YGR022C		SL	19.4	5	28.8	5
YGR054W		NLL	23.7	10	29.3	10
YGR055W	MUP1	NLL	24.3	15	27.0	25
YGR056W	RSC1	NSE	28.0	25	25.3	25
YGR057C	LST7	SL	18.4	5	32.8	5
YGR058W		SL	19.8	5	32.8	5
YGR059W	SPR3	NSE	28.8	25	25.3	25
YGR061C	ADE6	NSE	26.1	15	28.6	15
YGR064W		NSE	26.7	15	28.6	15
YGR066C		NLL	26.0	15	25.6	55
YGR067C		NSE	27.2	15	27.0	25
YGR068C		NSE	26.6	25	25.3	25
YGR069W		NSE	27.8	25	25.3	25
YGR070W	ROM1	NLL	25.9	15	25.6	55
YGR071C		SL*	13.8	5	32.8	5
YGR072W	UPF3	NLL	25.0	5	32.8	5
YGR077C	PEX8	SL	19.6	5	32.8	5
YGR078C	PAC10	NSE	26.7	15	27.0	25
YGR079W		NLL	22.6	10	29.3	10
YGR080W	TWF1	SL	17.4	5	32.8	5
YGR081C	SLX9	NLL	22.2	10	29.3	10
YGR084C	MRP13	NLL	24.6	5	32.8	5
YGR085C	RPL11B	NLL	22.0	5	32.8	5
YGR087C	PDC6	NLL	23.8	5	32.8	5
YGR088W	CTT1	NLL	25.5	15	28.6	15

YGR096W	TPC1	NLL	22.7	15	28.6	15
YGR097W	ASK10	NLL	23.7	10	29.3	10
YGR100W	MDR1	NLL	23.8	5	32.8	5
YGR101W	PCP1	SL	16.8	5	32.8	5
YGR104C	SRB5	NLL	22.2	5	32.8	5
YGR105W	VMA21	SL*	12.0	5	32.8	5
YGR107W		NSE	29.8	25	25.3	25
YGR108W	CLB1	NLL	25.1	15	28.6	15
YGR109C	CLB6	NLL	24.9	15	28.6	15
YGR111W		NLL	22.2	5	32.8	5
YGR112W	SHY1	SL	14.8	5	32.8	5
YGR118W	RPS23A	NSE	31.0	25	25.3	25
YGR121C	MEP1	NLL	24.3	10	29.3	10
YGR122W		NLL	23.9	10	29.3	10
YHR014W	SPO13	NLL	25.2	15	25.0	25
YHR015W	MIP6	NLL	20.8	5	22.4	5
YHR018C	ARG4	NSE	27.3	15	25.1	15
YHR021C	RPS27B	NLL	21.3	15	25.1	15
YHR022C		NLL	21.8	5	22.4	5
YHR028C	DAP2	NLL	22.0	5	22.4	5
YHR029C		NLL	21.0	5	22.4	5
YHR030C	SLT2	NLL	24.2	5	22.4	5
YHR031C	RRM3	SL	17.8	5	22.4	5
YHR033W		NLL	23.8	5	22.4	5
YHR034C	PIH1	SL		5		5
(YHR034W)			19.2		22.4	
YHR035W		NLL	22.0	5	22.4	5
YHR037W	PUT2	NLL	22.0	5	22.4	5
YHR038W	RRF1	NLL	23.8	5	22.4	5
YHR039C	MSC7	SL	18.6	5	22.4	5
YHR043C	DOG2	SL	19.8	5	22.4	5
YHR044C	DOG1	NLL	25.8	15	25.0	25
YHR046C	INM1	LL**	36.1	20	23.2	25
YHR047C	AAP1'	SL	15.8	5	22.4	5
YHR048W		NLL	23.6	5	22.4	5
YHR049C-A		NLL	24.4	5	22.4	5
YHR049W		NLL	23.8	5	22.4	5
YHR050W	SMF2	NLL	23.9	15	25.1	15
YHR057C	CPR2	NLL	24.0	5	22.4	5
YHR060W	VMA22	SL	12.6	5	22.4	5
YHR061C	GIC1	NLL	24.4	5	22.4	5
YHR066W	SSF1	LL**	38.5	20	24.6	65
YHR073W	OSH3	NLL	24.3	15	25.0	25
YHR075C	PPE1	NLL	25.7	15	25.0	25
YHR076W	PTC7	NLL	24.0	5	22.4	5
YHR077C	NMD2	NLL	24.0	5	22.4	5
YHR078W		NLL	21.0	5	22.4	5
YHR079C	IRE1	NLL	25.3	15	25.1	15
YHR080C		NLL	23.8	5	22.4	5
YHR081W	LRP1	NLL	24.4	5	22.4	5
YHR082C	KSP1	NSE	27.7	15	25.0	25
YHR086W	NAM8	NLL	23.8	5	22.4	5

YHR087W		NLL	23.1	15	25.0	25
YHR092C	HXT4	NLL	21.4	5	22.4	5
YHR093W	AHT1	NSE	28.4	15	25.0	25
YHR094C	HXT1	SL	17.4	5	22.4	5
YHR095W		SL	16.8	5	22.4	5
YHR096C		NSE	26.5	15	25.0	25
YHR097C		NSE	26.8	15	25.0	25
YHR100C		SL	15.0	5	22.4	5
YHR103W	SBE22	NLL	24.4	15	25.0	25
YHR104W	GRE3	SL	18.6	5	22.4	5
YHR105W	YPT35	NSE	28.8	25	24.6	65
YHR106W	TRR2	NLL	25.9	15	25.1	15
YHR108W	GGA2	NSE	26.6	15	25.0	25
YHR109W	CTM1	NLL	22.0	5	22.4	5
YHR110W	ERP5	SL	15.6	5	22.4	5
YHR111W	UBA4	SL	20.0	5	22.4	5
YHR112C		NLL	24.6	5	22.4	5
YHR113W		NSE	28.6	20	24.6	65
YHR114W	BZZ1	NLL	20.8	5	22.4	5
YHR115C		NLL	20.2	5	22.4	5
YHR116W		SL*	10.0	5	22.4	5
YHR117W	TOM71	NLL	24.6	5	22.4	5
YHR121W		NLL	24.4	5	22.4	5
YHR123W	EPT1	NLL	24.4	15	25.0	25
YHR124W	NDT80	NLL	24.2	5	22.4	5
YHR125W		NLL	20.6	5	22.4	5
YHR126C		SL	20.0	15	25.1	15
YHR129C	ARP1	SL	19.2	5	22.4	5
YHR130C		LL**	34.2	20	23.4	25
YHR132C	ECM14	NLL	22.2	5	22.4	5
YHR133C	NSG1	NLL	24.6	5	22.4	5
YHR134W	WSS1	SL	14.2	5	22.4	5
YHR135C	YCK1	NLL	23.4	5	22.4	5
YHR136C	SPL2	SL	15.6	5	22.4	5
YHR137W	ARO9	SL	20.0	5	22.4	5
YHR138C		NSE	26.7	15	25.1	15
YHR139C	SPS100	NSE	27.5	15	25.0	25
YHR139C-A		NSE	27.5	15	25.0	25
YHR142W	CHS7	SL	18.0	5	22.4	5
YHR143W	DSE2	SL	15.4	5	22.4	5
YHR151C		NSE	28.9	20	23.4	25
YHR152W	SPO12	NLL	24.2	5	22.4	5
YHR153C	SPO16	SL	17.0	5	22.4	5
YHR154W	RTT107	SL*	18.3	15	25.0	25
YHR155W		SL	19.4	5	22.4	5
YHR156C	LIN1	LL*	34.5	15	25.0	25
YHR157W	REC104	NSE	26.9	15	25.0	25
YHR158C	KEL1	NSE	26.8	15	25.0	25
YHR159W		NLL	22.0	5	22.4	5
YHR160C	PEX18	NLL	22.6	5	22.4	5
YHR161C	YAP1801	NLL	25.7	15	25.0	25
YHR163W	SOL3	NSE	28.9	15	25.0	25

YHR167W	THP2	SL	19.0	5	22.4	5
YHR178W	STB5	NLL	20.2	5	22.4	5
YHR179W	OYE2	SL	18.2	5	22.4	5
YHR182W		SL	17.2	5	22.4	5
YHR183W	GND1	NLL	24.2	5	22.4	5
YIL001W		NSE	33.7	15	27.3	15
YIL002C	INP51	NSE	29.7	15	27.3	15
YIL005W	EPS1	NLL	24.4	5	29.0	5
YIL056W		NLL	22.6	5	28.2	5
YIL085C	KTR7	NSE	26.3	15	26.7	15
YIL094C	LYS12	LL*	34.0	20	25.1	55
YIL102C		NLL	25.7	15	26.7	15
YIL111W	COX5B	NSE	26.9	15	26.7	15
YIL122W	POG1	NLL	22.3	10	27.0	10
YIL131C	FKH1	NSE	31.1	15	26.8	20
YIL136W	OM45	LL	34.5	20	26.2	20
YIL158W		NSE	26.5	15	26.2	20
YIR004W	DJP1	NSE	30.0	20	24.7	50
YJR034W	PET191	NLL	25.1	10	27.0	10
YJR039W		NLL	25.6	5	28.2	5
YJR044C	VPS55	NLL	25.1	15	26.7	15
YJR066W	TOR1	LL*	29.5	65	25.4	65
YKR045C		NSE	29.1	15	28.6	25
YKR047W		NLL	23.2	5	29.0	5
YKR048C	NAP1	NSE	27.6	15	27.3	15
YKR049C	FMP46	NSE	26.2	15	28.6	25
YKR050W	TRK2	SL	16.6	5	29.0	5
YKR051W		NLL	25.4	5	29.0	5
YKR052C	MRS4	SL	19.6	5	29.0	5
YKR054C	DYN1	NLL	24.6	10	27.4	10
YKR056W	TRM2	NLL	22.8	10	27.4	10
YKR057W	RPS21A	LL*	31.6	20	25.9	55
YKR058W	GLG1	NLL	25.8	5	29.0	5
YKR059W	TIF1	LL**	31.9	25	25.7	35
YKR060W	UTP30	NLL	20.6	5	29.0	5
YKR061W	KTR2	SL	15.4	5	29.0	5
YKR064W		NLL	26.0	15	28.6	25
YKR065C	FMP18	SL	18.8	5	29.0	5
YKR087C		SL*	9.2	5	28.8	5
YKR088C	TVP38	NLL	24.4	5	28.8	5
YKR089C		NLL	25.7	15	26.3	20
YKR090W	PXL1	NLL	23.2	5	28.8	5
YKR091W	SRL3	SL	18.4	5	28.8	5
YKR092C	SRP40	SL	16.2	5	28.8	5
YKR093W	PTR2	NLL	23.2	5	28.8	5
YKR097W	PCK1	NLL	20.2	5	28.8	5
YKR098C	UBP11	NLL	21.6	5	28.8	5
YKR099W	BAS1	LL**	36.6	20	26.3	20
YKR100C		NLL	20.8	5	28.8	5
YKR101W	SIR1	SL	19.4	5	28.8	5
YKR103W	NFT1	NLL	21.2	5	28.8	5
YKR104W	NFT1	NLL	22.4	5	28.8	5

YKR105C		LL	29.3	20	24.8	50
YLL018C-A	COX19	SL	17.4	5	28.8	5
YLR262C-A		NSE	27.3	15	26.3	20
YLR344W	RPL26A	NSE	29.1	15	26.8	20
YLR345W		NLL	22.4	10	27.0	10
YLR348C	DIC1	NLL	25.5	10	27.0	10
YLR349W		NSE	29.7	15	26.2	20
YLR350W	ORM2	NLL	22.6	5	28.2	5
YLR351C	NIT3	NSE	27.8	15	26.7	15
YLR352W		NLL	25.7	20	24.7	50
YLR353W	BUD8	NSE	32.5	20	24.7	50
YLR354C	TAL1	NSE	29.0	20	24.7	50
YLR356W		NLL	21.8	5	28.2	5
YLR357W	RSC2	SL	17.6	5	28.2	5
YLR360W	VPS38	NSE	31.9	15	26.2	20
YLR362W	STE11	SL	16.0	5	28.2	5
YLR363C	NMD4	LL	30.2	20	24.7	50
YLR364W		NSE	27.8	15	26.2	20
YLR365W		NLL	25.0	10	27.0	10
YLR366W		NSE	30.2	20	26.2	25
YLR367W	RPS22B	LL	30.2	20	24.7	50
YLR368W	MDM30	NSE	26.9	15	25.9	15
YLR371W	ROM2	LL**	40.7	15	27.1	15
YLR372W	SUR4	NLL	25.2	10	27.0	10
YLR373C	VID22	SL*	12.0	5	28.2	5
YLR374C		SL	16.0	5	28.2	5
YLR375W	STP3	NSE	26.8	15	26.2	20
YLR376C	PSY3	NLL	23.3	10	27.0	10
YLR377C	FBP1	NSE	28.3	20	24.7	50
YLR380W	CSR1	NLL	23.8	10	27.0	10
YLR381W	CTF3	NLL	25.2	5	28.2	5
YLR384C	IKI3	NLL	20.2	5	28.2	5
YLR385C		NSE	26.9	15	26.2	20
YLR386W	VAC14	SL	17.8	5	28.2	5
YLR387C		NSE	29.0	15	26.2	20
YLR388W	RPS29A	SL	19.4	5	28.2	5
YLR389C	STE23	NLL	25.5	10	27.0	10
YLR390W	ECM19	NLL	25.5	15	26.7	15
YLR422W		LL	32.6	20	26.3	20
YLR423C	ATG17	SL	18.4	5	28.8	5
YLR425W	TUS1	SL	17.6	5	28.8	5
YLR426W		SL	13.2	5	28.8	5
YLR427W	MAG2	NLL	23.8	5	28.8	5
YLR428C		NSE	27.5	15	26.3	20
YLR429W	CRN1	NSE	28.3	15	27.3	15
YLR431C	ATG23	NSE	27.0	15	26.3	20
YLR432W	IMD3	NSE	26.1	15	26.3	20
YLR433C	CNA1	NLL	25.3	15	26.3	20
YLR434C		NLL	22.8	5	28.8	5
YLR436C	ECM30	NSE	29.1	15	26.3	20
YLR437C		NLL	22.3	15	26.3	20
YLR438W	CAR2	SL	16.4	5	28.8	5

YLR441C	RPS1A	LL*	35.2	20	26.3	20
YLR443W	ECM7	SL	13.0	5	28.8	5
YLR444C		NLL	23.5	15	26.3	20
YLR445W		SL*	13.0	5	28.8	5
YLR446W		NLL	24.2	5	28.8	5
YLR447C	VMA6	SL*	12.0	5	28.8	5
YLR448W	RPL6B	LL*	30.7	30	24.7	70
YLR449W	FPR4	NLL	20.6	5	28.8	5
YLR450W	HMG2	SL	19.0	5	28.8	5
YLR452C	SST2	LL	31.0	25	25.7	25
YLR453C	RIF2	NLL	24.3	15	26.3	20
YLR454W	FMP27	NLL	24.9	15	26.3	20
YLR456W		NLL	21.6	5	28.8	5
YLR460C		NLL	20.3	15	26.3	20
YLR461W	PAU4	NSE	29.5	15	26.3	20
YML009C	MRPL39	NLL	21.9	15	26.3	20
YML009C-A		NLL	25.7	20	26.3	20
YML021C	UNG1	SL	15.8	5	28.8	5
YML081C-A	ATP18	SL**	7.6	5	28.8	5
YMR052C-A		NLL	25.8	15	26.2	20
YMR052W	FAR3	NLL	25.8	10	27.0	10
YMR053C	STB2	LL	37.5	15	26.8	15
YMR054W	STV1	NLL	25.0	15	26.7	15
YMR055C	BUB2	NLL	24.1	10	27.0	10
YMR056C	AAC1	NSE	28.2	20	24.7	50
YMR057C		NSE	29.7	20	24.7	50
YMR058W	FET3	NLL	21.8	5	28.2	5
YMR060C	TOM37	SL	17.2	5	28.8	5
YMR158C-B		SL	19.6	5	28.8	5
YMR169C	ALD3	NLL	23.6	5	28.8	5
YMR174C	PAI3	NSE	28.8	15	26.3	20
YMR175W	SIP18	SL**	16.5	10	27.3	15
YMR194C-A		NLL	21.4	5	28.8	5
YMR326C		SL	15.6	5	28.8	5
YNL229C	URE2	LL**	32.0	20	24.4	40
YNR032C-A	HUB1	NLL	23.6	5	28.8	5
YNR050C	LYS9	LL*	31.2	20	24.8	50
YNR051C	BRE5	LL*	31.9	20	24.8	50
YNR056C	BIO5	NLL	20.8	5	28.8	5
YNR057C	BIO4	NLL	21.8	5	28.8	5
YNR058W	BIO3	NSE	29.9	20	24.8	50
YNR059W	MNT4	NLL	23.8	5	28.8	5
YNR060W	FRE4	NLL	22.2	5	28.8	5
YNR061C		NSE	28.0	15	26.3	20
YNR062C		NLL	25.7	15	26.3	20
YNR063W		NLL	22.4	5	28.8	5
YNR064C		SL	18.2	5	28.8	5
YNR065C	YSN1	NLL	24.8	5	28.8	5
YNR066C		SL*	14.0	5	28.8	5
YNR067C	DSE4	NSE	26.5	15	26.3	20
YNR068C		SL	12.4	5	28.8	5
YOR008C-A		NSE	27.4	15	26.3	20

YOR097C		NSE	30.6	25	25.3	25
YOR099W	KTR1	NLL	23.5	10	29.3	10
YOR100C	CRC1	LL*	31.6	25	25.3	25
YOR101W	RAS1	LL*	34.9	20	27.4	35
YOR104W	PIN2	NLL	23.6	5	32.8	5
YOR105W		NLL	25.3	25	25.3	25
YOR106W	VAM3	SL*	14.4	5	32.8	5
YOR107W	RGS2	LL**	34.2	25	25.3	25
YOR108W	LEU9	NSE	27.3	15	27.0	25
YOR109W	INP53	LL**	32.0	45	24.5	45
YOR111W		NSE	28.9	20	25.4	65
YOR112W		NLL	25.8	25	25.3	25
YOR113W	AZF1	NSE	28.3	15	28.6	15
YOR114W		NLL	25.8	5	32.8	5
YOR115C	TRS33	NLL	25.3	10	29.3	10
YOR118W		NSE	27.9	15	25.6	55
YOR120W	GCY1	NSE	26.5	15	25.1	20
YOR121C		NLL	21.2	5	32.8	5
YOR123C	LEO1	NSE	26.7	15	27.0	25
YOR124C	UBP2	NSE	28.5	15	27.0	25
YOR126C	IAH1	NLL	24.2	5	32.8	5
YOR129C		SL	18.0	5	32.8	5
YOR130C	ORT1	NSE	27.7	15	28.6	15
YOR131C		NLL	23.7	10	29.3	10
YOR132W	VPS17	NLL	25.8	5	32.8	5
YOR133W	EFT1	NLL	24.2	5	32.8	5
YOR134W	BAG7	NSE	30.3	20	25.4	65
YOR135C		LL	31.0	20	25.4	65
YOR136W	IDH2	LL**	34.6	20	26.3	55
YOR137C	SIA1	NSE	29.5	15	28.6	15
YOR138C	RUP1	NLL	21.8	5	32.8	5
YOR139C		NLL	25.6	10	29.3	10
YOR140W	SFL1	NLL	24.7	15	28.6	15
YOR142W	LSC1	NLL	23.9	10	29.3	10
YOR144C	ELG1	NLL	25.0	5	32.8	5
YOR152C		NLL	21.8	5	32.8	5
YOR153W	PDR5	NLL	23.1	10	29.3	10
YOR154W		NLL	25.6	5	32.8	5
YOR156C	NFI1	NLL	23.1	10	29.3	10
YOR161C		NLL	22.9	10	29.3	10
YOR162C	YRR1	NSE	28.7	15	29.4	25
YOR163W	DDP1	NSE	27.8	25	25.3	25
YOR164C		NLL	22.6	5	32.8	5
YOR165W	SEY1	SL	16.6	5	32.8	5
YOR166C		NSE	32.5	15	28.6	15
YOR167C	RPS28A	NSE	28.8	25	25.3	25
YOR170W		NLL	23.3	10	29.3	10
YOR171C	LCB4	NSE	29.9	20	25.4	65
YOR172W	YRM1	NSE	29.8	15	28.6	15
YOR173W	DCS2	NLL	22.8	10	29.3	10
YOR175C		NLL	22.9	10	29.3	10
YOR177C	MPC54	NSE	31.5	15	28.6	15

YOR178C	GAC1	NLL	23.3	10	29.3	10
YOR179C	SYC1	NSE	28.5	15	28.6	15
YOR180C	DCI1	NSE	29.4	15	28.6	15
YOR182C	RPS30B	NLL	22.4	5	32.8	5

Supplemental Table 2. Genes corresponding to single-gene deletion strains classified as potentially long-lived (LL) from a screen of 564 single-gene deletion strains for mutations that increase replicative life span. A minimum of 15 mother cells were assayed for replicative life span from each deletion strain shown. Strains were obtained from the *MATα* yeast ORF deletion collection. Verification studies were carried out by examining the replicative life span for at least 40 mother cells from the corresponding deletion mutant contained in the *MAT***a** ORF deletion collection. In some cases, the gene deletion was re-generated in the *MATα* parental strain, BY4742, and replicative life span was assayed for at least 40 mother cells. Data shown represents the percent effect on mean replicative life span and Wilcoxon Rank-Sum test p-values for each mutant relative to wild type (BY4742 for *MATα* cells and BY4741 for *MAT***a** cells) cells contained in the same experiment. Shaded rows represent genes that met verification criteria (**see Supplemental Methods**) for increased replicative life span upon deletion.

		MATα Deletion Set		MATa Deletion set		Remake in BY4742	
ORF	Gene	% Effect	p-value	% Effect	p-value	% Effect	p-value
YKR099W	BAS1	38	0.01	-8	0.18		
YNR051C	BRE5	29	0.02	30	0.01		
YOR100C	CRC1	25	0.02	3	0.67		
YDR110W	FOB1	21	0.01	ND	ND	42	< 0.001
YOR136W	IDH2	31	0.003	18	0.02		
YHR046C	INM1	56	0.001	-10	0.03		
YOR109W	INP53	31	0.001	8	0.62		
YDR315C	IPK1	41	0.001	1	0.83		
YHR156C	LIN1	38	0.02	10	0.35		
YIL094C	LYS12	36	0.04	4	0.86	-18	0.03
YNR050C	LYS9	26	0.02	8	0.84		
YLR363C	NMD4	22	0.08	-33	< 0.001		
YIL136W	OM45	33	0.07	-12	0.12		
YDR313C	PIB1	32	0.05	14	0.11	-15	0.04
YOR101W	RAS1	27	0.03	-10	0.42		
YBR267W	REI1	38	< 0.001	47	< 0.001	52	< 0.001
YOR107W	RGS2	35	0.002	-9	0.13		
YLR371W	ROM2	49	0.001	16	0.05		
YDL075W	RPL31A	35	0.02	59	< 0.001		
YLR448W	RPL6B	23	0.09	33	< 0.001	23	0.01
YLR441C	RPS1A	35	0.01	3	0.6		
YKR057W	RPS21A	22	0.04	10	0.35		
YLR367W	RPS22B	22	0.07	-8	0.09		
YDR477W	SNF1	36	0.07	-13	0.02		
YHR066W	SSF1	56	0.002	9	0.33		
YLR452C	SST2	21	0.07	4	0.79		
YMR053C	STB2	40	0.06	-26	< 0.001		
YKR059W	TIF1	24	0.008	4	0.37		
YJR066W	TOR1	23	0.01	22	0.004	21	0.04

YNL229C	URE2	15	0.1	21	0.02		
YDR247W	VHS1	31	0.03	0	0.4		
YBR238C		25	0.01	34	0.002	21	0.02
YBR255W		34	0.002	25	0.002	19	0.02
YBR266C		37	< 0.001	47	< 0.001		
YDR124W		27	0.01	-11	0.08		
YDR248C		17	0.03	-5	0.24		
YDR274C		25	0.05	-10	0.04		
YDR307W		31	0.006	-2	0.7		
YER186C		27	0.05	-3	0.33		
YER187W		48	0.004	-5	0.14		
YHR130C		58	< 0.001	-6	0.21		
YKR105C		18	0.08	-3	0.47		
YLR422W		25	0.09	-5	0.23		
YOR135C		22	0.07	18	0.02		

Fig. S1

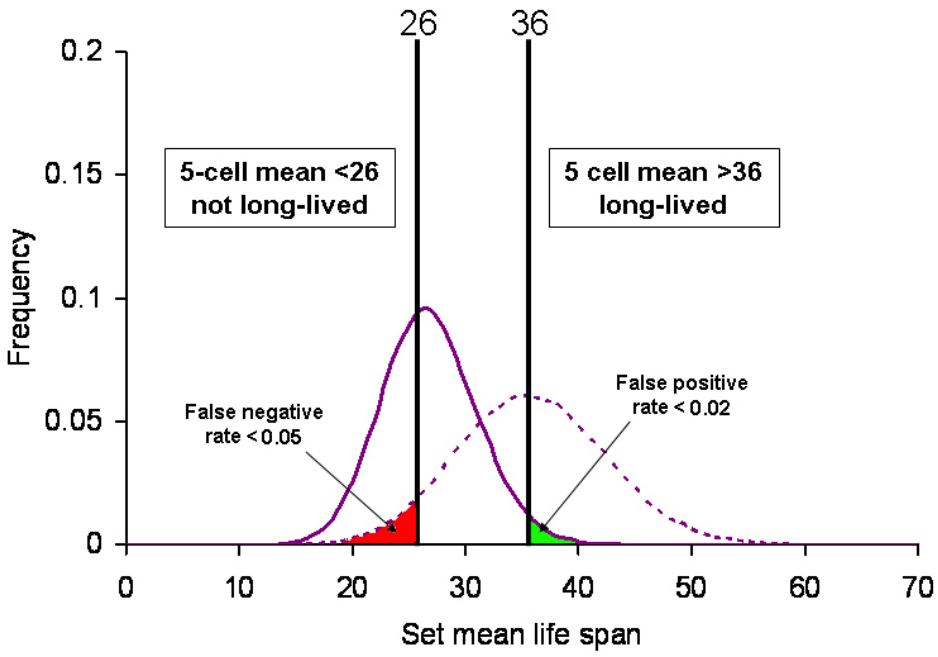

Supplemental Figure 1. Iterative process to identify long-lived mutants based on the theoretical 5-cell set mean life span distributions for wild-type cells (solid line) and long-lived (broken line) cells. Mean life span distributions for the 5-cell sets were generated computationally by randomly selecting 100,000 5-cell sets from experiment derived replicative life span data sets for wild-type and long-lived cells. For each mutant analyzed, if the 5-cell mean life span is less than 20, the strain is classified as short-lived (SL), since the 5-cell mean life span for wild-type should be less than 20 fewer than 5% of the time ($p < 0.05$). If the 5-cell mean life span is less than 26, the strain is classified as not long-lived (NLL), with an expected false negative rate of 0.05. If the 5-cell mean life span is greater than 36, the strain is classified as potentially long-lived (LL), with an expected false negative rate of 0.02. Strains not classified after 5-cells are subjected to another round of replicative life span analysis on 5 additional cells, with the same criteria applied. Strains not classified after 2 rounds are subjected to a third round of 5-cell replicative life span analysis followed by p-value determination on the pooled data (N at least 15 cells) using a Wilcoxon Rank-Sum test against experiment-matched wild type cells.

Fig. S2

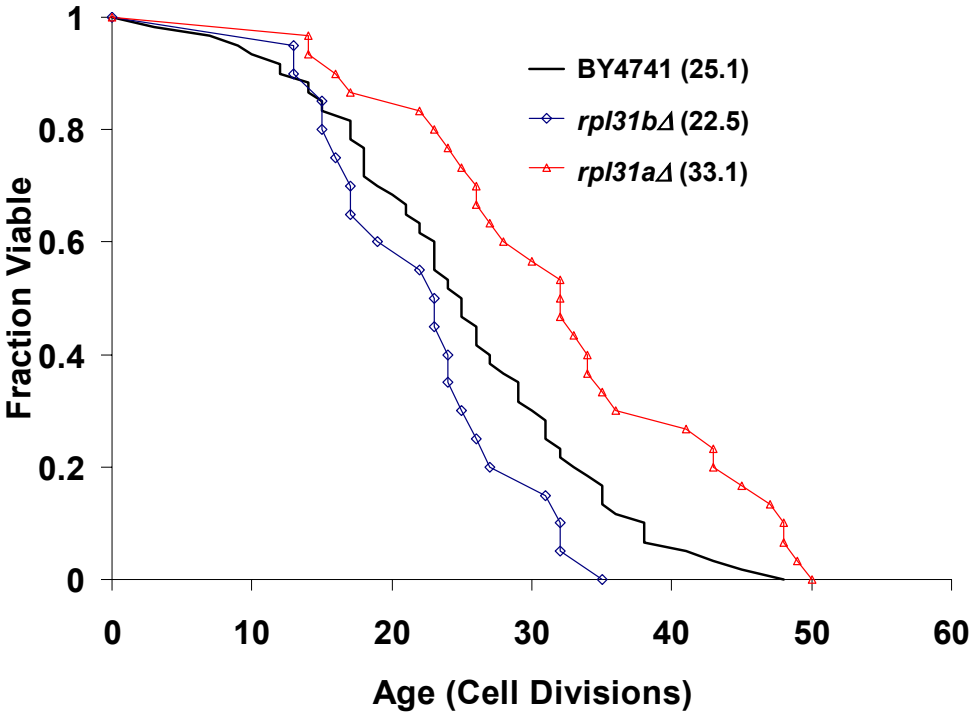

Supplemental Figure 2. Ribosomal gene paralogs can have different roles in replicative life span determination. Deletion of *RPL31A* increases life span while deletion of *RPL31B* does not.

Fig. S3

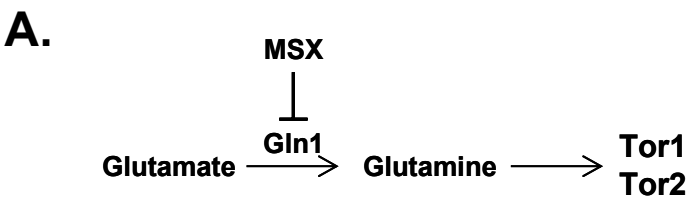

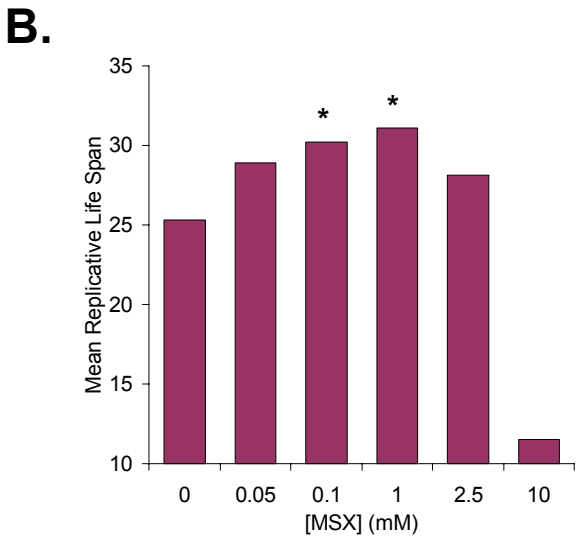

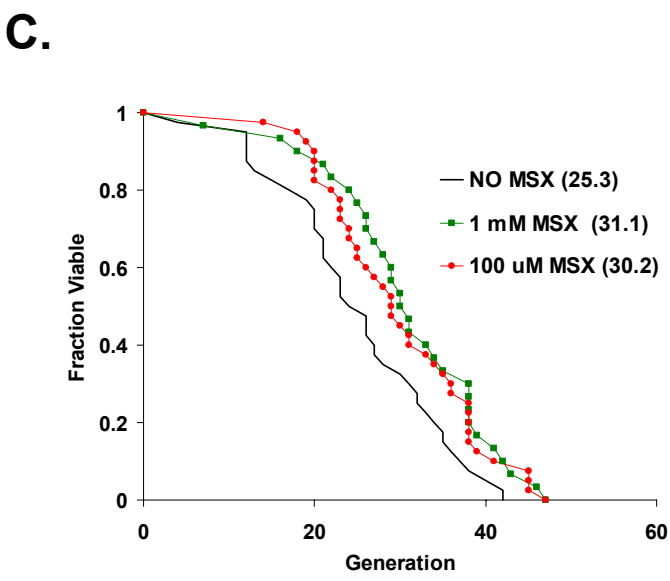

Supplemental Figure 3. Methionine sulfoximine (MSX) increases replicative life span. A. MSX inhibits TOR by decreasing intracellular glutamine levels. B. Treatment of cells with the TOR inhibitor MSX increases replicative life span of BY4742 mother cells in a dose-dependent manner, up to 2.5 mM. At concentrations higher than 2.5 mM MSX dramatically shortens life span due to a profound growth defect. C. A statistically significant increase in life span was observed at 0.1 mM and 1 mM MSX. Life span was determined for 40 cells at each concentration of MSX.